PNAS

Supporting Information for
Regulatory sites in the Mon1-Ccz1 complex control Rab5 to Rab7 transition and endosome maturation

Ann-Christin Borchers[1], Maren Janz[2], Jan-Hannes Schäfer[3], Arne Moeller[3], Daniel Kümmel[4], Achim Paululat[2], Christian Ungermann[1,5*], and Lars Langemeyer[1,5*]

[1]Osnabrück University, Department of Biology/Chemistry, Biochemistry section, 49076 Osnabrück, Germany

[2]Osnabrück University, Department of Biology/Chemistry, Zoology and Developmental Biology section, 49076 Osnabrück, Germany

[3]Osnabrück University, Department of Biology/Chemistry, Structural Biology section, 49076 Osnabrück, Germany

[4]University of Münster, Institute of Biochemistry, 48149 Münster, Germany

[5]Center of Cellular Nanoanalytics (CellNanOs), Osnabrück University, 49076 Osnabrück, Germany

Lars Langemeyer and Christian Ungermann
Email: lars.langemeyer@uos.de (L.L.), cu@uos.de (C.U.)

This PDF file includes:

Detailed Material & Methods

Strains and Plasmids

Strains used in this study are listed in Table S1. Genetic manipulation of yeast strains including deletion and tagging of genes was performed using a PCR-product- and homologous recombination-based approach described in (1). Plasmids used in this study are listed in Table S2.

Expression and purification of Rab GTPases and prenylation machinery components

GST-TEV-Rab5, GST-TEV-Rab7, GST-TEV-Ypt10, GST-TEV-Ypt7 and the components of the prenylation machinery, Bet4, His-TEV-Bet2, His-Sumo-*D.m.* GDI, GST-PreSc-Gdi1 and Mrs6-His were expressed and purified as before (Table S2)(2). *E. coli* BL21 Rosetta cells were transformed with 100 ng plasmid DNA and grown in LB media to an OD_{600}=0.6 at 37 °C. Protein expression was induced using 0.25 mM IPTG for 14 h at 16 °C. Cells were harvested and lysed in 50 mM HEPES-NaOH, pH 7.5, 150 mM NaCl, 1.5 mM $MgCl_2$, 1 mM DTT, 1 mM PMSF and 0.05x Protease inhibitor cocktail (PIC; a 20X stock solution contained 2 µg/ml Leupeptin, 10 mM 1,10-Phenanthroline, 10 µg/ml Pepstatin A and 2 mM Pefablock) using the microfluidizer (Microfluidics, Westwood, MA, U.S.A). Yeast and *Drosophila* Rab GTPases were either purified as GST-fusion constructs by Glutathione elution for use in GST pull downs or as Tag-free version by overnight cleavage with TEV protease. *S.c.* GST-PreSc-Gdi1 was purified by PreScission protease (PreSc) cleavage. Bet4 His-TEV-Bet2, Mrs6-His, and His-Sumo-*D.m.* GDI were added to Ni-NTA agarose from cleared lysates and eluted with 300 mM imidazole in elution buffer. The GST-PreSc-Gdi1 construct was cleaved for 2 h at 16 °C in the presence of 0.5 mM DTT. Proteins eluted with imidazole or glutathione were dialyzed overnight against buffer with 50 mM HEPES-NaOH, pH 7.5, 150 mM NaCl and 1.5 mM $MgCl_2$ with one buffer exchange. To remove the His-Tag from His-Sumo-*D.m.* GDI, the dialyzed protein was incubated with SUMO protease for 2 h at 4 °C, and protease was then removed using Ni-NTA beads. Proteins were aliquoted, snap frozen in liquid nitrogen, and stored at -80 °C. The purity and efficiency of the purifications was analyzed by SDS gel electrophoresis.

Expression and purification of *Drosophila* GEF complexes in Sf21 cells

Drosophila Mon1-Ccz1 and Mon1-Ccz1-Bulli were expressed using the biGBac system (3) and purified as described (2). Briefly, Sf21 cells were grown as a monolayer culture in Insect-XPRESS Protein-free Insect Cell Medium (Lonza, Cologne, Germany) in standard T175 culture flasks at 27 °C. Viral infection was performed for 72 h. Cells were then harvested at 500 *g* for 5 min, resuspended in buffer containing 50 mM HEPES-NaOH, pH 7.5, 300 mM NaCl, 1 mM $MgCl_2$, 10% (v/v) glycerol, 1 mM PMSF, and 0.05x PIC and lysed using the microfluidizer (Microfluidics,Westwood, MA. U.S.A) or via homogenization. The cleared lysate was incubated for 2 h with Glutathione 4B Sepharose (GE Healthcare, Solingen, Germany) followed by washing of the Sepharose with 50 mM HEPES-NaOH, pH 7.5, 300 mM NaCl, 1,5 mM $MgCl_2$, and 10% glycerol and overnight cleavage of protein in the presence of 1 m DTT and 0.4 mg/ml PreSc protease. The next morning, protein was eluted and concentrated to 500 µl using a Vivaspin6 10,000 MVCO centrifugal concentrator (Sartorius, Göttingen, Germany). The concentrated sample was subjected to size exclusion chromatography using an Äkta FPLC UPC-900 liquid chromatography system (Cytiva, Freiburg im Breisgau, Germany) equipped with a Superdex 200 increase 10/300 GL column (Cytiva, Freiburg im Breisgau, Germany) and buffer containing 50 mM HEPES-NaOH, pH 7.5, 300 mM NaCl, 1 mM $MgCl_2$, and 10 % (v/v) glycerol. Peak fractions were collected and analyzed by SDS-PAGE.

Tandem-Affinity Purification

Purification of yeast Mon1-Ccz1 was essentially performed as described (4) with all centrifugation steps conducted at 4 °C. Three liters of culture were grown in YPG to an OD_{600}=2-3 at 30 °C. Cells were harvested at 4000 *g*, and once washed in ice cold H_2O. Pellets were resuspended in equal amounts of buffer containing 50 mM HEPES-NaOH, pH 7.4, 150 mM NaCl, 1.5 mM $MgCl_2$, 5 % (v/v) glycerol, 1x FY, 0.5 mM PMSF and 0.5 mM DTT and were dropwise snap frozen in liquid nitrogen. Drops were then subjected to cryomill lysis, and powder was resuspended in equal amount of buffer on a nutator. Lysate was centrifuged for 10 min at 3200 *g* and then for 70 min at 125,000 *g*. Supernatant was incubated for 1.5 h at 4 °C with IgG Sepharose (Cytiva, Freiburg im Breisgau, Germany) equilibrated with buffer containing 50 mM HEPES-NaOH, pH 7.4, 150 mM NaCl, 1.5 mM $MgCl_2$ and 5 % glycerol. Beads were washed extensively, and the protein was cleaved overnight at 4 °C in buffer with 1 mM DTT and TEV protease. Proteins containing fractions were analyzed on SDS gels followed by Coomassie staining.

In vitro prenylation of yeast and *Drosophila* Rab GTPases

Prenylated yeast and *Drosophila* Rab-REP and Rab-GDI complexes were generated as described in (2, 5). For the generation of *Drosophila* Rab7-GDI, the yeast prenylation machinery and the *Drosophila* GDI were used. Rab proteins were either loaded with GDP (REP-complexes, Merck, Darmstadt, Germany) or MANT-GDP (GDI-complexes; Jena Bioscience, Jena, Germany) prior to the prenylation reaction in prenylation buffer containing 50 mM HEPES-NaOH, pH 7.4, 150 mM NaCl, and 1.5 mM $MgCl_2$.

In solution and membrane-associated fluorescent nucleotide exchange assays

In solution nucleotide exchange factor assays were essentially performed as in (6) with minor changes. Purified Ypt7/Rab7 were loaded with MANT-GDP (GDI-complexes, Jena Bioscience, Germany) in the presence of 20 mM HEPES/NaOH, pH 7.4, and 20 mM EDTA for 30 min at 30 °C. Bound nucleotide was stabilized with 25 mM $MgCl_2$. 2 µM Rab were incubated with varying amounts of GEF in a SpectraMax M3 Multi-Mode Microplate Reader (Molecular Devices, San Jose, CA, USA) and after baseline stabilization, nucleotide exchange was triggered by 0.1 mM GTP (for *D.m.* GEFs) or 1 mM GTP (*S.c.* GEFs). MANT-GDP release following Rab activation was monitored over time using an excitation wavelength of 355 nm and emission at 448 nm. Data after 10 min initial signal decrease were fitted individually against a first-order exponential decay using OriginPro9 software (OriginLab Corporation, Northampton, USA) and k_{obs} (s^{-1}) was determined as 1/t1. K_{obs} was then plotted against the GEF concentration, and k_{cat}/K_M ($M^{-1}s^{-1}$) was derived as the slope of the resulting linear fit.

The liposome-based GEF assays were performed as described (2) with liposomes with a vacuolar mimicking composition (7) with 47.6 mol % dioleoyl phosphatidylcholine (DLPC 18:2 18:2), 18 % dioleoyl phosphatidylethanolamine (DLPE 18:2 18:2), 18 % soy phosphatidylinositol (PI), 1 % diacylglycerol (DAG 16:0 16:0), 8 % ergosterol, 2 % dioleoyl phosphatidic acid (DLPA 18:2 18:2), 4.4 % dioleoyl phosphatidylserine (DLPS 18:2 18:2), 1 % dipalmitoyl PI(3)phosphate (PI(3)P diC16) (Avanti Polar Lipids, Inc., Alabaster, AL, U.S.A) and extruded to 400 nm using a polycarbonate filter and a hand extruder (Avanti Polar Lipids, Inc., Alabaster, AL, U.S.A). Liposomes were decorated with 150 nM prenylated recruiter GTPase in the presence of 200 µM GTP and 1.5 mM EDTA for 15 min at RT. The loading reaction was stopped with 3 mM $MgCl_2$, and the mix was transferred to a half micro cuvette 109.004F-QS with 10 x 4 mm thickness (Hellma, Müllheim, Germany). 250 nM Rab7/Ypt7-GDI were added and the cuvette was filled up to

800 µl with prenylation buffer omitting the volume of the GEF. The cuvette was placed in a fluorimeter (Jasco, Gross-Umstadt, Germany) at 30 °C with the wavelengths mentioned above. After baseline stabilization, the indicated concentration of GEF was added to trigger nucleotide exchange, and fluorescence decrease was monitored over time. GEF assays with artificial recruitment of His-tagged GEF complexes to liposomes using His-tagged Bulli-MC1 was performed essentially as above. 3 mol% DOGS-NTA (18:1 18:1) were included into liposomes and corrected for by adjustment of DLPC amounts. The measurements were performed in a SpectraMax iD3 Multi-Mode Microplate Reader (Molecular Devices, San Jose, CA, U.S.A). Data were individually fitted against a first-order exponential decay using OriginPro9 software (OriginLab Corporation, Northampton, MA, U.S.A) and k_{obs} (s^{-1}) was determined as 1/t1. Values of the mutant analysis were normalized to the respective wt value in the measurement and statistical comparison was made using a using a two-sample student's t-test assuming equal variances.
All kinetic parameters of used GEF complexes are listed in Table S3.

Statistical interpretation

The P-values for each statistical analysis were interpreted as the following: $P > 0.5$ = not significant (n.s.), $P < 0.05$ = *, $P < 0.01$ = **, $P < 0.001$ = ***, $P < 0.0001$ = ****.

Liposome sedimentation assay

Membrane association of GEF complexes was analyzed via liposome sedimentation. Liposomes containing the lipid composition also used for the nucleotide exchange assays including 0.5 % ATTO550 (AD 550, ATTO-TEC, Siegen, Germany) were loaded with recruiter GTPase as described for the membrane-associated fluorescent nucleotide exchange assay. As control, the Rab GTPase was omitted. After 8 min preincubation at 30 °C, 12.5 nM GEF complex was added and sample was incubated for 15 min. Liposomes were sedimented at 20000 *xg* for 20 min at 4 °C. Presence of GEF was detected using SDS page and Western Blot with an anti-FLAG M2 antibody (1:1000, F3165, Merck, Darmstadt, Germany) and a fluorescence-coupled secondary antibody (1:10000, SA5-35521, Thermo Fisher Scientific, Dreieich, Germany). Band intensity was analyzed using Fiji software (National Institutes of Health, Bethesda, MD, U.S.A) and normalized to the respective input.

GST Rab pull downs

75 µg GST-tagged Rab GTPase was loaded with either 10 mM GDP or GTP (Sigma-Aldrich, Taufkirchen, Germany) in the presence of 20 mM EDTA and 50 mM HEPES-NaOH, pH 7.4 at 30 °C for 30 min. The nucleotide was stabilized using 25 mM $MgCl_2$, and protein was incubated for 1 h at 4 °C with 30 µl GSH sepharose (Cytiva, Freiburg im Breisgau, Germany) equilibrated with 50 mM HEPES-NaOH, pH 7.4, 150 mM NaCl, 1.5 mM $MgCl_2$ in the presence of 7 mg/ml BSA. Then the beads were spun for 1 min, and the supernatant was discarded. Next, 25 µg Mon1-Ccz1, 7 mg/ml BSA and 1 mM nucleotide were added, and the tube was filled up to 300 µl with pull down buffer containing 50 mM HEPES-NaOH, pH 7.4, 150 mM NaCl, 1 mM $MgCl_2$, 5% (v/v) Glycerol and 0.1% (v/v) Triton X-100, and incubated 1.5 h at 4 °C on a turning wheel. Then beads were washed 3x using pull down buffer. Subsequently, bound protein was eluted from the beads for 20 min at RT in a turning wheel using 300 µl elution buffer with 50 mM HEPES-NaOH, pH 7.4, 150 mM NaCl, 20 mM EDTA, 5% (v/v) Glycerol and 0.1% (v/v) Triton X-100. Eluted fraction was TCA-precipitated, and 20 % of it was analyzed by SDS page and Western Blot together with 1 % input sample. Mon1 was detected using a Mon1-antibody (1:1000, Ungermann lab) and a fluorescence-coupled secondary antibody (#SA5-35571, 1:10000, Thermo Fisher Scientific, Dreieich, Germany). For the Rab GTPase as loading control, 1x Laemmli buffer was added to the GSH beads after elution, and samples were boiled for 10 min at 95 °C. 2 % of each loading control was loaded onto SDS page and stained with Coomassie Brilliant blue G250. Band intensity was quantified using Fiji software (National Institutes of Health, Bethesda, MD) and normalized to the respective input. Significance was determined using a using a two-sample student's t-test assuming equal variances.

Pho8Δ60 assay

The assay was essentially performed as in (8). Yeast strains expressing a genetically truncated version of the *PHO8* gene (Pho8Δ60) were grown in YPAD media overnight at 30 °C. The next morning, cells were diluted to an OD_{600}=0.2 in 10 ml and grown until logarithmic phase. Then cells were centrifuged, washed in starvation media (0.17% yeast nitrogen base without amino acids or ammonium sulfate and 2 % glucose), and starvation was induced for indicated time periods. Then 5 OD equivalents of cells were harvested and washed in H_2O. As control, 5 OD equivalents of cells grown in YPAD were treated the same. Pellets were resuspended in buffer 20 mM PIPES, pH 6.8, 0.5% Triton X-100, 50

mM KCl, 100 mM potassium acetate, 10 mM $MgCl_2$, 10 µM $ZnSO_4$ and 2 mM PMSF and cells were lysed by glass bead lysis in the FastPrep-24 (MP Biomedicals, Eschwege, Germany). Pho8 activity was monitored by incubation of 200 µl lysate with 50 µl buffer 250 mM Tris–HCl, pH 8.5, 0.4% Triton X-100, 10 mM $MgCl_2$, 10 µM $ZnSO_4$ and 1.25 mM p-nitrophenyl phosphate and the colorimetric reaction was measured in a SpectraMax M3 Multi-Mode Microplate Reader (Molecular Devices, San Jose, CA, USA) at OD_{400}.The enzymatic activity was calculated by the linear method. The slopes of the experimental samples were normalized to the ALP activity of WT cells under nutrient rich conditions and displayed in arbitrary units (A.U.). Significance was determined using a one-way ANOVA with a Tukey post-hoc test using OriginPro9 software (OriginLab Corporation, Northampton, USA).

Analysis of yeast and *Drosophila* protein expression

To test the expression of Rab GTPases Vps21 and Ypt7 in yeast cells, 4 OD units were harvested and resuspended in buffer containing 0.2 M NaOH and 30 mM β-mercaptoethanol. Proteins were precipitated by adding TCA to a final concentration of 15 % and analyzed via SDS PAGE and Western Blotting. Antibodies against Vps21 (1:1000) and Ypt7 (1:3000) were generated in the Ungermann lab, the Tom40 antibody (1:2000) was a gift of the Neupert lab. Primary antibodies were detected with secondary antibody goat anti-Rabbit IgG (H+L) Secondary Antibody, DyLight™ 800 4X PEG, (#SA5-35571, 1:10000; Thermo Fisher Scientific, Dreieich, Germany) or DyLight™ 680 (#35568, 1:10000; Thermo Fisher Scientific, Dreieich, Germany). The expression of UAS-driven wild-type Mon1::HA and truncated $Mon1^{\Delta 100}$::HA in transgenic flies using the ubiquitous *daughterless*-GAL4 driver was verified by western blot of *Drosophila* whole cell lysate using standard protocols. Actin staining was used as a loading control. As a primary antibody rabbit α-HA (H6908, 1:1000, Sigma-Aldrich,St. Louis, MO, U.S.A, RRID:AB_260070) and mouse α-Actin (1:10, DSHB, clone JLA20) was used, combined with a secondary antibody α-rabbit-alkaline phosphatase (A3687, 1:10,000, Sigma-Aldrich, St. Louis, MO, U.S.A ,RRID:AB_258103) and α-mouse-alkaline phosphatase (A3562, 1:10000, Sigma-Aldrich, , St. Louis, MO, U.S.A, RRID:AB_258091).

Fluorescence microscopy of yeast cells

For yeast fluorescence microscopy, cells were grown overnight in synthetic media containing 2 % (w/v) glucose and essential amino acids (SDC+all). In the morning, cells

were diluted to an OD_{600}=0.1 and grown to logarithmic phase. Vacuoles were stained with FM4-64 (Thermo Fisher Scientific, Dreieich, Germany) where indicated. 1 OD equivalent of cells was resuspended in 50 µl SDC+all containing 30 µM FM4-64 and incubated at 30 °C for 20 min. Cells were washed twice with fresh media and incubated with 500 µl fresh SDC+all for another 45 minutes at 30°C. Cells were imaged on an Olympus IX-71 inverted microscope (DeltaVision Elite, GE Healthcare, Solingen, Germany) equipped with a 100x NA 1.49 objective, a sCMOS camera (PCO, Kelheim, Germany), an InsightSSI illumination system, SoftWoRx software (Applied Precision, Issaquah, WA, U.S.A.) and GFP, mCherry and Cy5 filters. Stacks with 0.25 µm or 0.35 µm spacing sampling the whole cell volume were taken. Where indicated, z-stacks for constrained-iterative deconvolution (SoftWoRx) were performed. Microscopy images were processed as single slices and quantified using Fiji software (National Institutes of Health, Bethesda, MD, U.S.A). One representative slice is shown in the figures.

The mNeon-Ypt7- and mCherry-Vps21-positive dots in the Mon1 truncation mutant (Figure 2C and 2E) were manually counted in the whole cell volume for n>50 cells. Statistical analysis was done using a two-sample student's t-test assuming equal variances.

For the analysis of the vacuolar rim localization of mNeon-Ypt7 (Figure 3I), a line profile was placed across the FM4-64-stained vacuole in the focus section and signal intensity in both channels was detected. Both values were averaged and the ratio of FM4-64 and Ypt7 signal was determined for n>50 cells. Significance of the values was determined in a one-way ANOVA with a Tukey post-hoc test using OriginPro9 software (OriginLab Corporation, Northampton, USA).

Growth test

Yeast cells were incubated in YPD media overnight at 30 °C. In the morning, cultures were diluted and grown to logarithmic phase at 30 °C. Then cells were diluted to an initial OD_{600}=0.25 in YPD, and spotted in 1:10 serial dilutions onto control and selection plates and incubated for several days at the indicated temperature. Each day, plates were imaged to monitor growth.

Fly stocks

The following fly stocks were obtained from the Drosophila stock center at Bloomington: *da*-GAL4 (RRID:BDSC_55850) and w^{1118} (RRID:BDSC_5905). *handC*-GAL4 was

previously generated by us (9). The UAS-Mon1::HA line was obtained from T. Klein, Düsseldorf, Germany (10) and the UAS-Mon1$^{\Delta 100}$::HA line was generated in this study. Fly husbandry was carried out as described previously (11).

Generation of the transgenic UAS-Mon1$^{\Delta 100}$::HA line

To generate a Mon1$^{\Delta 100}$::HA construct in a *Drosophila* vector suitable for establishing transgenic fly lines, a Mon1$^{\Delta 100}$-cDNA was used as a PCR template (Source DNA clone IP03303 from the *Drosophila* Genomics Resource Center (DGRC, Bloomington, IN, USA)). Via overlap PCR, the Mon1$^{\Delta 100}$ construct was fused to an HA-tag following by a PCR to generate restriction sites (XhoI and EcoRI) for insertion into an injection plasmid. Therefore, the following PCR primers were used: 5' TACCGGAATTCATGGAGGAGGAATACGATTACCAGC '3 (forward) and 5' TACCGC TCGAGTTAAGCGTAATCTGGAACG '3 (reverse). The PCR amplicon was purified, digested with EcoRI and XhoI and cloned into pYED (12). The UAS-Mon1$^{\Delta 100}$::HA expression plasmid was injected into RRID:BDSC_24749 for integration at 86Fb on the 3rd chromosome (13). A commercial service was used for establishing transgenic fly lines (BestGene, Chino Hills, CA, USA).

FITC-Albumin Uptake

FITC-albumin uptake assays were performed in pericardial nephrocytes as described previously with minor modifications (14). Briefly, 3rd instar larvae, in which Mon1::HA or Mon1$^{\Delta 100}$::HA was expressed in nephrocytes using *hand*C-GAL4 as a driver, were anesthetized fixed ventral side upwards on Sylgard 184 silicone elastomer plates using minute pins. Specimens were always covered by artificial hemolymph. All internal organs except for the pericardial cells and associated tissue (e.g. heart, alary muscles) were removed. Preparation buffer was replaced by fresh artificial hemolymph buffer containing 0.2 mg/ml FITC-albumin (A9771, Albumin–fluorescein isothiocyanate conjugate, MW: 66 kDa; Sigma-Aldrich, Taufkirchen, Germany), and specimens were incubated in the dark for 5 min or 10 min. Uptake was stopped by fixation in 8 % paraformaldehyde (PFA) in phosphate-buffered saline (PBS) followed by two washing steps with PBS. Subsequently, tissues were embedded in Fluoromount-G mounting medium containing DAPI (Thermo Fisher, Waltham, MA, USA) for microscopic analysis. Uptake efficiency was quantified by imaging respective nephrocytes (LSM800, Zeiss, Jena, Germany). Imaging settings were identical for wild-type Mon1 and Mon1$^{\Delta 100}$ mutant animals, and the

mean pixel-intensity measurement function provided by the Fiji software package was used to quantify uptake efficiency (15). Mean pixel intensity was calculated in relation to the perimeter of the cell. An unpaired, two-tailed student's t-test was used for statistical analysis using GraphPad Prism 9 (Boston, MA, U.S.A).

Immunohistochemistry

3rd instar larvae expressing *handC* driven wild-type Mon1::HA and truncated Mon1$^{\Delta 100}$::HA were dissected in PBS and fixed with 4 % paraformaldehyde (PFA) in PBS for one hour at RT. After three washing steps of 10 min, specimens were permeabilized with 1 % Triton X-100 in PBS for one hour at RT, followed by three further washing steps with BBT (0.1 % BSA and 0.1 % Tween-20 in PBS) for 10 min each. Subsequently, specimens were incubated for 30 min in a blocking solution containing 1 % BSA and 0.1 % Tween-20 in PBS followed by incubation with the primary antibodies (rabbit anti-Rab5, 1:250, Abcam Cat# ab31261, RRID:AB_882240, Cambridge, United Kingdom; mouse anti-Rab7, 1:10, Developmental Studies Hybridoma Bank Cat# Rab7, RRID:AB_2722471, University of Iowa, IA, USA (16)) in BBT overnight at 8 °C. Samples were rinsed three times with BBT (10 min, RT), blocked with blocking solution for 30 min and incubated with secondary antibodies (anti-rabbit Alexa Fluor 488, 1:200, Jackson ImmunoResearch Laboratories, Inc, West Grove, PA, U.S.A, ((Code Number: 115-165-003, RRID:AB_2338680); anti-mouse Cy3, 1:200, Dianova GmbH, Eching, Germany) in BBT for two hours at RT followed by three washing steps with BBT. Samples were embedded in Fluoromount-G mounting medium containing DAPI (Thermo Fisher, Waltham, MA, USA). Confocal images were captured with a laser scanning microscope (LSM800, Zeiss, Jena, Germany) equipped with a Zeiss EC Plan-Neofluar 40x / NA 1.30 Oil DIC M27 40x objective, Multikali PMT detector and Zen2.6 software. Filters for Alexa Fluor 488, Cy3 and DAPI were used and 0.37 µm stacks were taken. Deconvolution was then performed using the Regularized Inverse Filter (RIF) algorithm implemented in the Zen2.6 software.Image processing was done with Fiji and Affinity Photo (Serif, Nottingham, United Kingdom).

Measurement of Rab5 structures in nephrocytes

To analyze the size and number of Rab5-positive vesicles in nephrocytes, the 'Intermodes' auto threshold implemented in Fiji was used to highlight Rab5 dots above the set threshold. Two sections of each cell (one from the periphery, one from the center of the cell) were then analyzed using the 'analyzed particle' function resulting in the number and

size of Rab5 dots. The mean size of Rab5 dots per cell and the number per 100 μm^2 cell area were calculated. An unpaired, two-tailed student's t-test was used for statistical analysis using GraphPad Prism 9 (Boston, MA, U.S.A).

Transmission electron microscopy

Briefly, specimens were prepared in PBS and subsequently fixed for 4 h at RT in fixative (2% glutaraldehyde (Sigma-Aldrich, Taufkirchen, Germany)/ 4% paraformaldehyde (Merck, Darmstadt, Germany) in 0.05 M cacodylate buffer pH 7.4). Next, specimens were post-fixed for 2 h at RT in 1% osmium tetroxide in 0.05 M cacodylate buffer pH 7.4 (Sciences Services, Munich, Germany) and dehydrated stepwise in a graded ethanol series followed by 100% acetone. Subsequently, specimens were embedded in Epon 812 and polymerized for 48 h at 60 °C. Ultrathin sections (70 nm) were cut on an ultramicrotome (UC6 and UC7 Leica, Wetzlar, Germany) and mounted on formvar-coated copper slot grids. Sections were stained for 30 minutes in 2% uranyl acetate (Sciences Services, Munich, Germany) and 20 minutes in 3 % lead citrate (Roth, Karlsruhe, Germany). A detailed protocol for processing nephrocytes for TEM analysis can be found elsewhere (17). All samples were analyzed at 80 kV with a Zeiss 902, and Zeiss LEO912 and at 200 kV with a Jeol JEM2100-Plus transmission electron microscope (Zeiss, Jena, Germany; Jeol, Tokyo, Japan).

Modeling of the yeast Mon-Ccz1 complex bound to Ypt7 and Ypt10

With the sequences of Mon1, Ccz1, Ypt7 and Ypt10, an initial model of the tetrameric complex was generated using AlphaFold2 multimer (18). The switch regions of nucleotide-free Ypt7 were manually edited based on the crystal structure of the catalytic MC1-Ypt7 core complex (6) and GTP and Mg^{2+} were added to the Ypt10 nucleotide binding pocket. Only regions that were modeled with high confidence are shown in the figures.

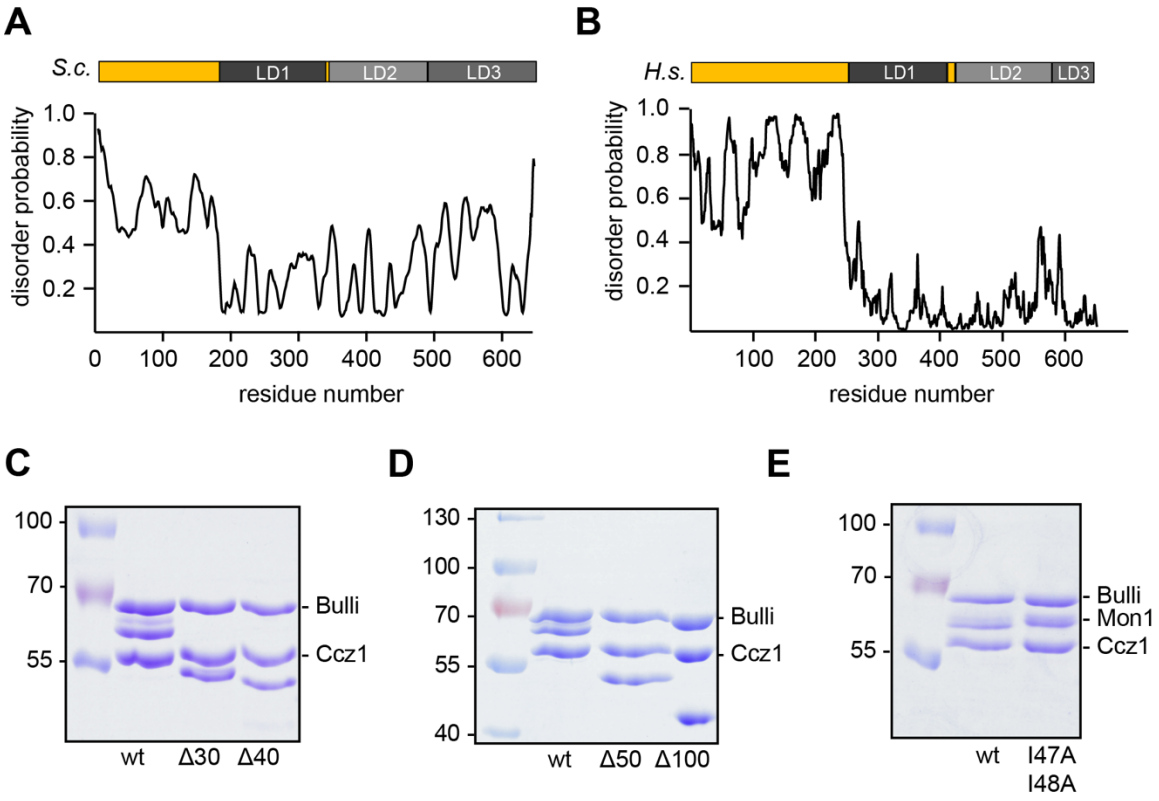

Figure S1. Analysis of the Mon1 N-terminal region. (A,B) The N-terminal regions of *S.c.* and *H.s.* Mon1 are disordered. Disorder probability of each residue of *S.c.,* (A) and *H.s.*, (B) Mon1 was determined using IUPred2A web interface (44, 45). Longin domains (LD) 1-3 are highlighted in grey shades. Values >0.5 are considered as disordered. **(C-E)** Expression of truncated Mon1 (Mon1$^{\Delta 1\text{-}30}$, Mon1$^{\Delta 1\text{-}40}$, **C**), and (Mon1$^{\Delta 1\text{-}50}$, Mon1$^{\Delta 1\text{-}100}$, **D**) and of hydrophobic patch mutant (Mon1$^{I47,\ 48A}$, **E**) does not affect complex stability of Trimeric Mon1-Ccz1-Bulli complex. GEF complexes were purified as described in the method section and analyzed by SDS-PAGE and Coomassie staining.

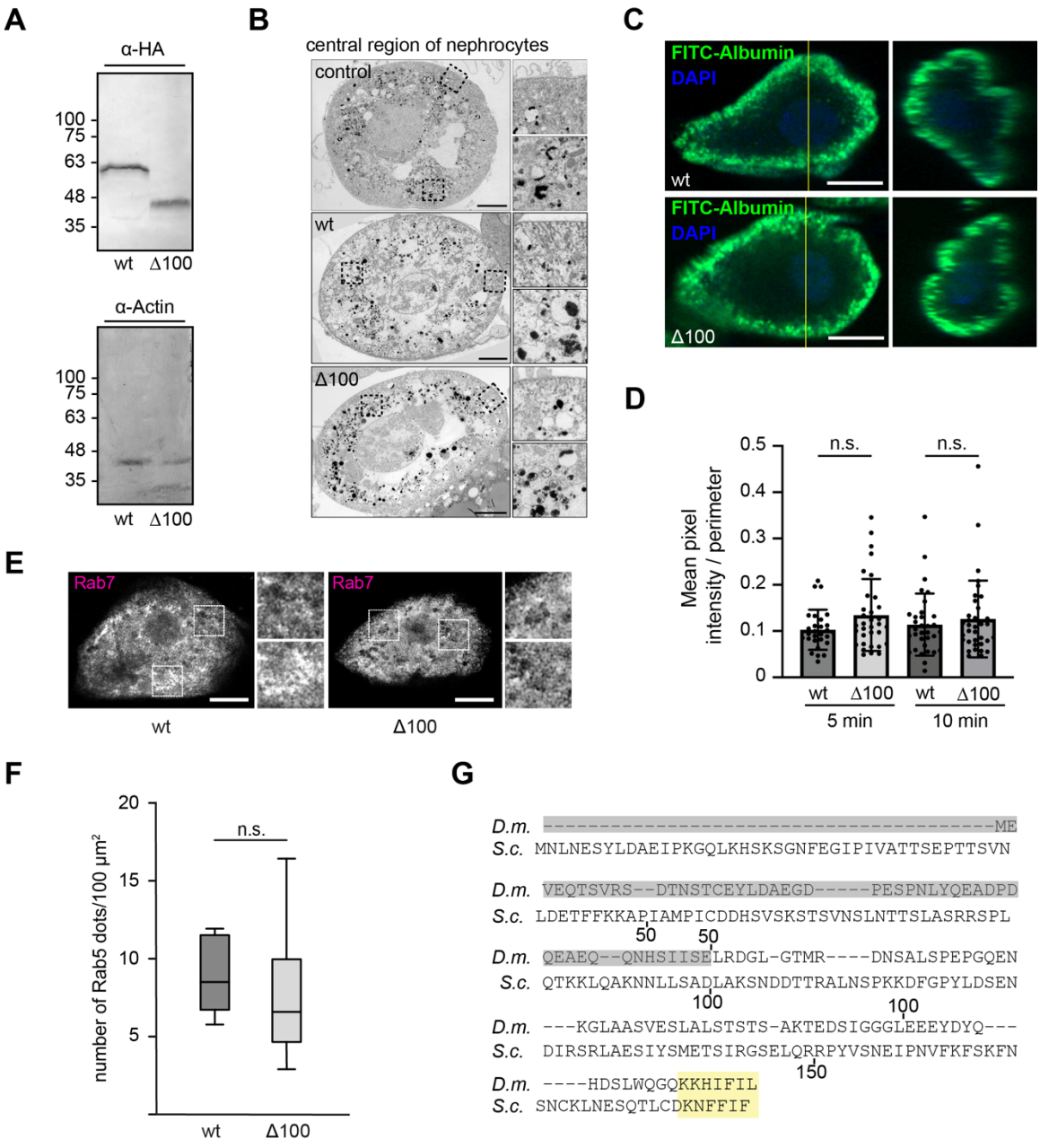

Figure S2. Analysis of N-terminal mutations in *D. melanogaster* Mon1. (**A**) Protein levels of wild-type Mon1 and Mon1$^{\Delta 100}$ in adult female flies using the *daughterless*-GAL4 driver. Mon1 was detected via its HA-tag using α-HA (rabbit). Actin staining with α-Actin (mouse) served as loading control. (**B**) TEM images of control nephrocytes (3rd instar larvae from the crossing *handC*-GAL4 crossed to *white*^{1118}) and nephrocytes from 3rd instar larvae expressing wildtype or Mon1$^{\Delta 100}$ under control of the *handC*-GAL4 driver. Enlargements show the labyrinth channel system with slit diaphragm and clathrin coated vesicles. Further, endocytic vesicles with electron dense material are shown. (**C**) Uptake

of FITC-Albumin (molecular weight of approximately 66 kDa) within nephrocytes from 3rd instar larvae expressing wild-type Mon1 or Mon1$^{\Delta 100}$ under control of the *handC*-GAL4 driver. DAPI was used to visualize nuclei. Right panel shows an orthogonal view of the cells at the position marked with a yellow line. Size bar, 10 µm. (**D**) Quantification of FITC-Albumin uptake in nephrocytes for 5 min and 10 min. Regions of interest were analyzed for the mean pixel intensity in relation to the perimeter of the cell. For wild-type Mon1, 28 cells from 10 animals (5 min) and 33 cells from 11 animals (10 min) were quantified. For Mon1$^{\Delta 100}$, 33 cells from 11 animals (5 min) and 35 cells from 12 animals were quantified (10 min). (P-value n.s.>using unpaired, two sample student´s t-test). **(E)** Localization of endogenous Rab7 in *Drosophila* nephrocytes from 3rd instar larvae expressing wild type or Mon1Δ100 under the control of the *handC*-GAL4 driver. An antibody against Rab7 was used. Optical sections show the distribution of Rab7 in detail. Size bar: 10 µm. **(F)** Analysis of the number of Rab5 dots / 100 µm^2 cell area calculated from 15 cells from three animals for wild-type Mon1 and 13 cells from four animals for Mon1$^{\Delta 100}$ (n.s.: not significant using an unpaired, two sample student´s t-test). **(G)** Alignment of *D.m.* and *S.c.* Mon1 N-terminal region. *D.m.* Mon1$^{\Delta 50}$ (grey) corresponds to truncation of residues 1-100 in the *S.c.* protein. The beginning of LD1 is marked in yellow. Alignment was done with Clustal omega web interface (Sievers et al., 2011; Goujon et al., 2010).

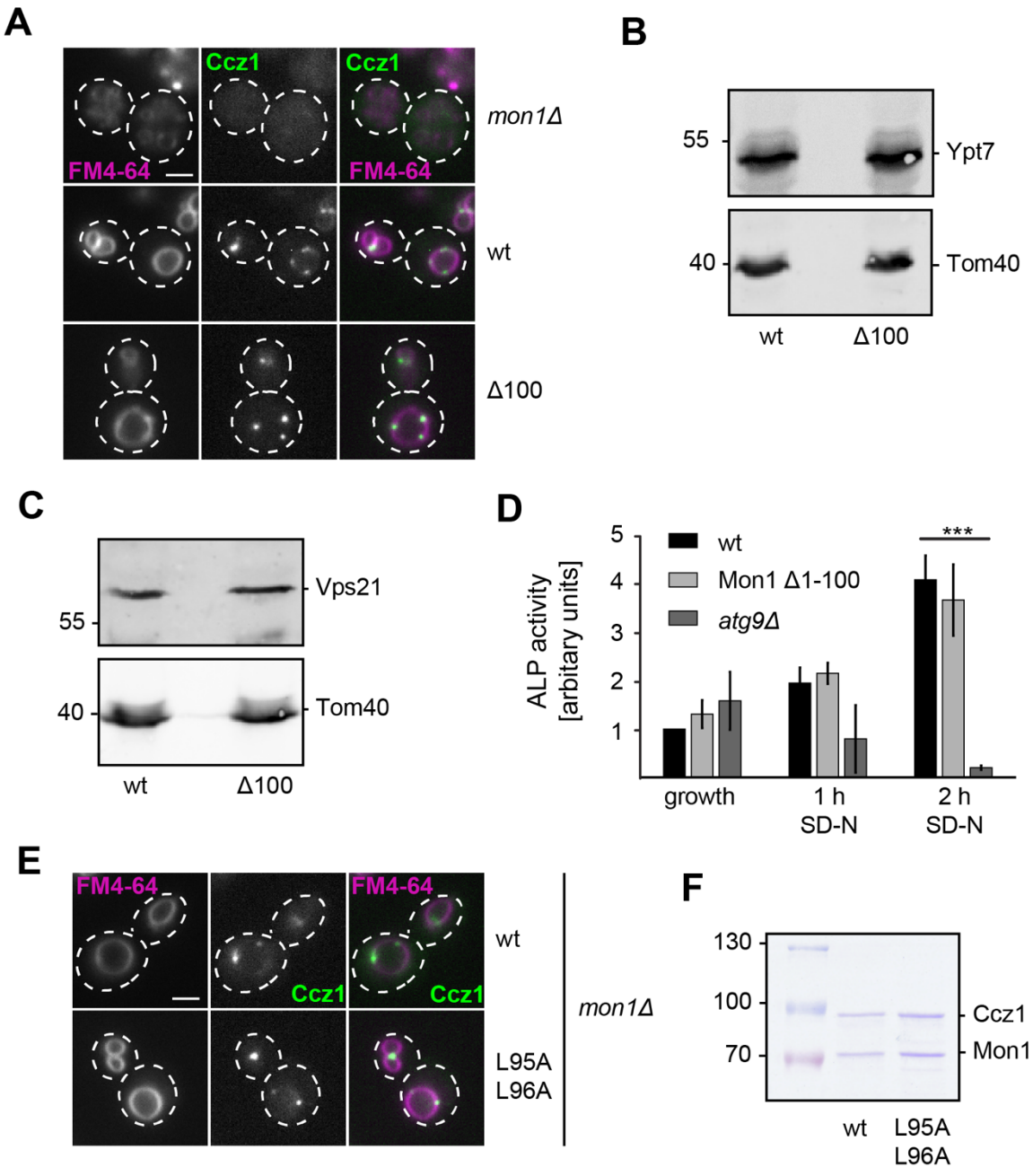

Figure S3. Analysis of N-terminal mutations in *S. cerevisiae* Mon1. (A) Truncation of the Mon1 N-terminal does not affect Ccz1- localization. Localization of Ccz1-mNeon in yeast cells in a *mon1* deletion strain or in the presence of endogenously expressed wild type or Mon1$^{\Delta 100}$ using fluorescence microscopy. Vacuoles were stained with FM4-64. Size bar, 2 µm. One representative slide from a z-stack is shown. **(B,C)** Expression control of endosomal Rab GTPases Ypt7 (B) and Vps21 (C) analyzed in Fig. 2C and 2E. Expression in cell lysate was analyzed using 1 OD unit (Ypt7) or 4 OD units (Vps21) loaded onto SDS gel for subsequent western blotting. Protein was visualized using

antibodies against Ypt7 and Vps21. Tom40 decoration served as loading control. **(D)** Analysis of autophagic flux. Autophagic flux was analyzed in the indicated strains using the PhoΔ60 assay, for details see methods. (P-value for *atg9*Δ cells over wild-type after 2h starvation *** $p<0.001$ using one-way ANOVA with a Tukey post-hoc test). **(E)** Mutation of the Mon1 hydrophobic patch does not affect Ccz1- localization. Plasmids encoding $Mon1^{wt}$ or $Mon1^{L95AL96A}$ were expressed under their endogenous promoter in a *mon1* deletion strain. Vacuoles were stained with FM4-64. Size bar, 2 µm. One representative slide from a z-stack is shown. **(F)** Analysis of purified Mon1-Ccz1 complex with mutation of $Mon1^{L95A,L96A}$. GEF complexes were purified as described in the method section and analyzed by SDS-PAGE and Coomassie staining.

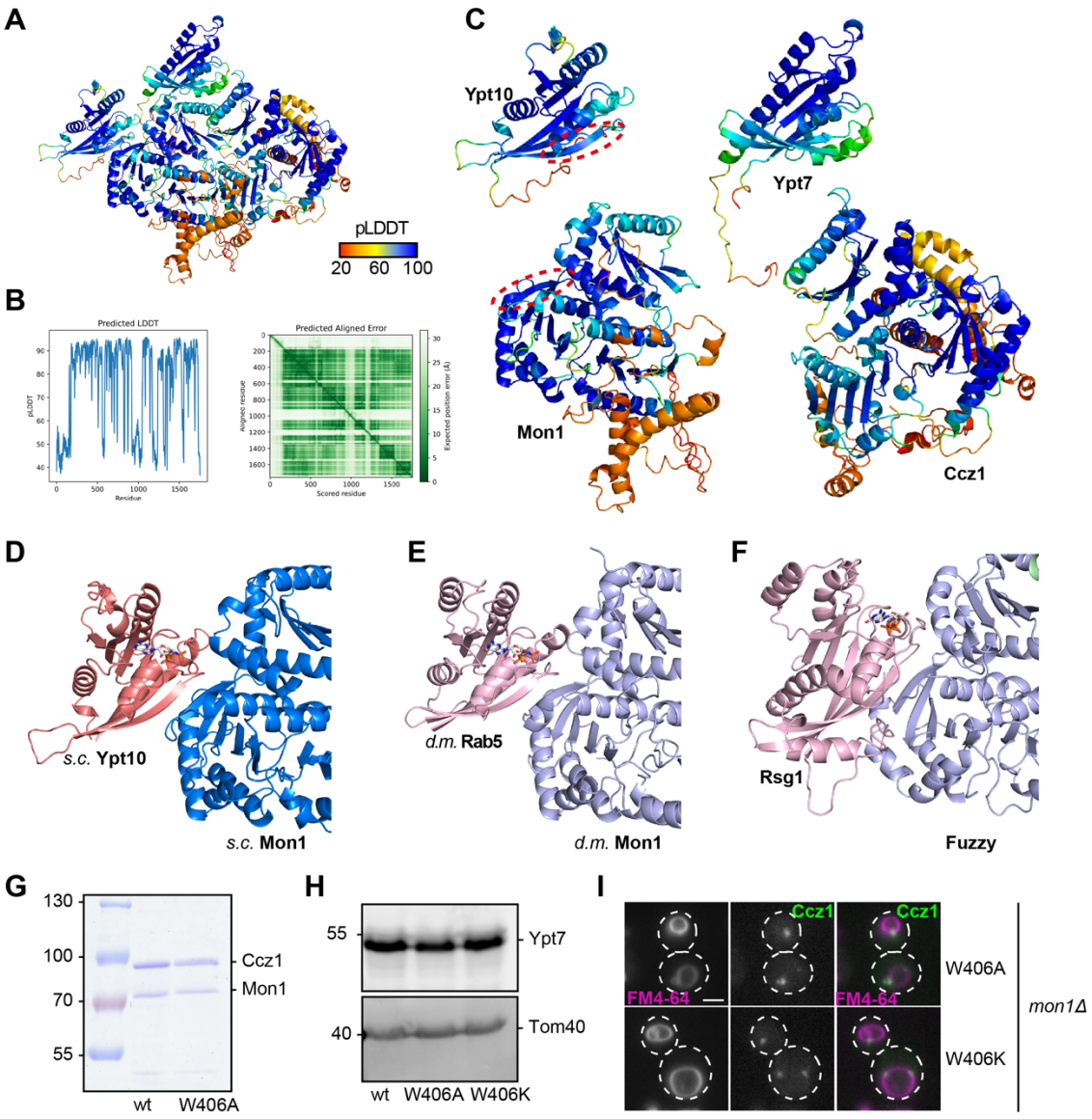

Figure S4. Analysis of the binding interface between Mon1 and the Rab5-like Ypt10 protein.

(**A**) Carton representation of the *S.c.* Mon1-Ccz1-Ypt7-Ypt10 complex model color-coded according to the pLDDT values. (**B**) Plots of the per-residue local confidence score (on a scale from 0 – 100) and of the predicted aligned error (PAE). (**C**) Carton representation of the modelled complex subunits color-coded according to the pLDDT values. The proposed binding interfaces of Mon1 and Ypt10 are highlighted. (**D**) Close-up of the modeled *S.c.* Mon1-Ypt10 interface (**E**), the modeled *D.m.* Mon1-Rab5 interface, and (**F**) the Fuzzy-

Rsg1 interface observed in the cryo-EM structure of CPLANE (18) are shown in the same orientation. **(G)** Analysis of the GEF complex containing Mon1^{W406A}. GEF complexes were purified using tandem-affinity purification and analyzed by SDS-PAGE and Coomassie staining. (**H**) Expression level of Ypt7 in Figure 3I is not affected by Mon1 mutation. Expression of mNeon-Ypt7 in cell lysate of wildtype and Mon1^{W406} mutants was analyzed using 1 OD unit cells loaded onto an SDS gel for subsequent western blotting. Protein was visualized using an antibody against Ypt7, Tom40 expression served as loading control. **(I)** Mutations in Mon1 do not affect Ccz1- localization. Plasmids encoding Mon1^{W406A} or Mon1^{W406K} were expressed under the endogenous Mon1 promoter in a *mon1* deletion background. Vacuoles were stained with FM4-64. Size bar, 2 µm. One representative slide from a z-stack is shown.

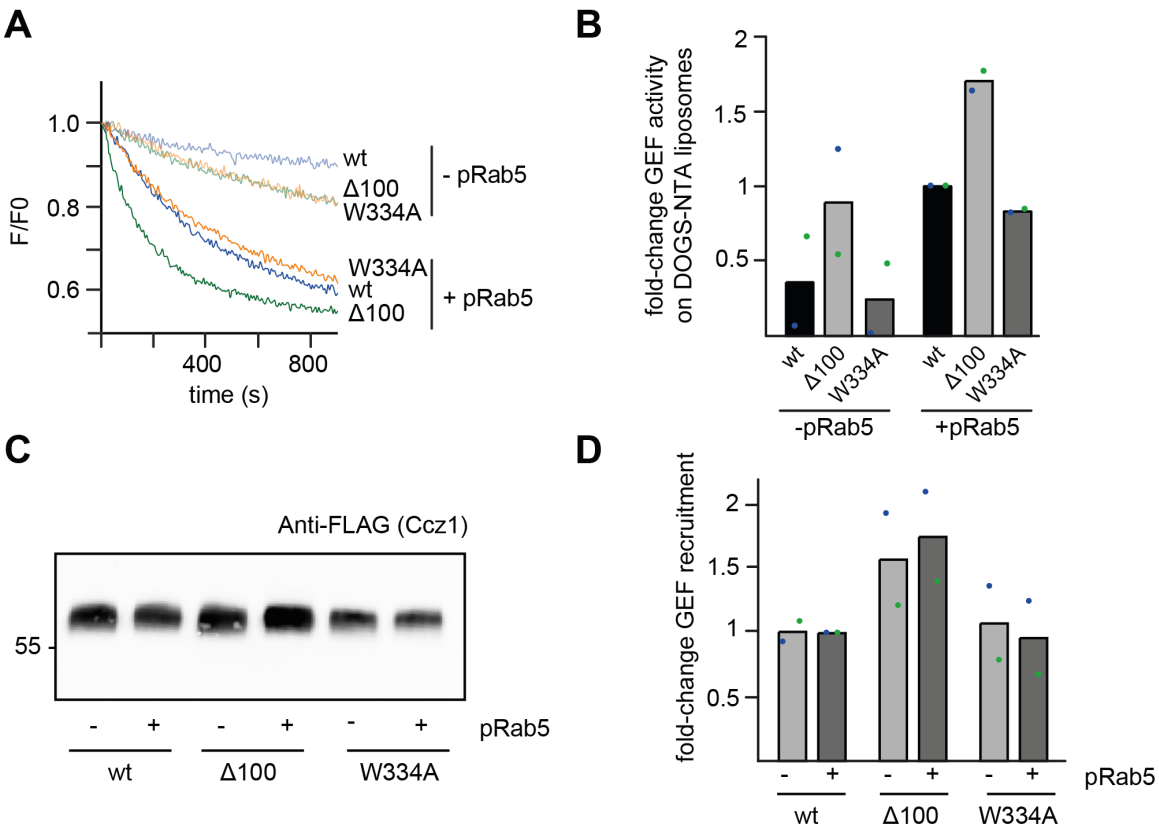

Figure S5. Artificial tethering of Mon1-Ccz1-Bulli to membranes (**A**) On liposome GEF assay of Mon1^{wt}, Mon1$^{\Delta 1\text{-}110}$ and Mon1^{W334A} containing the MC1 trimer with Bulli-His$_6$ with artificial GEF recruitment. Liposomes containing 3 mol% DOGS-NTA were preloaded with 150 nM prenylated Rab5 in the presence of 200 µM GTP and 1.5 mM EDTA. As control, the Rab GTPase was omitted. The nucleotide was stabilized using 3 mM $MgCl_2$. 250 nM Mant-GDP loaded Rab7:GDI were added and nucleotide exchange was started by adding 25 nM wild-type (blue), Mon1$^{\Delta 1\text{-}110}$ mutant (green) or Mon1^{W334A} mutant (orange) GEF complex. Decrease in fluorescence was measured over time and normalized to fluorescence upon GEF addition. (**B)** Comparison of fold-change in GEF activity of (A). k_{obs} of each curve was determined as described in the method section and k_{obs} values of mutants were normalized to the wild-type value in the presence of Rab5. Bar graphs represent average fold-change and dots represent individual changes from two experiments. (**C)** Artificial recruitment of GEF complexes for on-liposome GEF assay. After the measurement in (A), the whole reaction was centrifuged for 20 min at 20,000 *g*. Pellet fractions were analyzed by SDS page and western blot using anti-FLAG antibody. (**D)** Quantification of GEF complex recruitment. Analysis was performed as in C and band intensities were quantified using Fiji. Values were normalized to wt value with Rab5-

decorated liposomes. Bar graphs represent average fold-change in GEF recruitment and dots represent individual changes from two experiments.

Table S1. Yeast strains used in this study

Strains	Genotype	Reference
CUY11940	MATα *leu2-3,112 ura3-52 his3-Δ200 trp-Δ901 lys2-801 suc2-Δ9 GAL ypt7Δ::natNT2 URA3::pRS406-YPT7pr-mNeon-(GGSG)x3-YPT7-YPT7term*	(2)
CUY13443	MATα *leu2-3,112 ura3-52 his3-Δ200 trp-Δ901 lys2-801 suc2-Δ9 GAL ypt7Δ::natNT2 URA3::pRS406-YPT7pr-mNeon-(GGSG)x3-YPT7-YPT7term MON1Δ1-100::KanMX-Mon1pr*	This study
CUY13585	MATα *leu2-3,112 ura3-52 his3-Δ200 trp-Δ901 lys2-801 suc2-Δ9 GAL ypt7Δ::natNT2 URA3::pRS406-YPT7pr-mNeon-(GGSG)x3-YPT7-YPT7term VPS21::hphNT1-PHO5pr-3xmCherry*	This study
CUY13586	MATα *leu2-3,112 ura3-52 his3-Δ200 trp-Δ901 lys2-801 suc2-Δ9 GAL ypt7Δ::natNT2 URA3::pRS406-YPT7pr-mNeon-(GGSG)x3-YPT7-YPT7term MON1Δ1-100::KanMX-MON1pr VPS21::hphNT1-PHO5pr-3xmCherry*	This study
CUY10489	MATα *his3Δ1 leu2Δ0 lys2Δ0 ura3Δ0 pho13Δ::KAN pho8::PHO8Δ60*	Reggiori Laboratory
CUY10490	MATα *his3Δ1 leu2Δ0 lys2Δ0 ura3Δ0 pho13Δ::KAN pho8::PHO8Δ60 atg9Δ::URA*	Reggiori Laboratory
CUY13880	MATα *his3Δ1 leu2Δ0 lys2Δ0 ura3Δ0 pho13Δ::KAN pho8::PHO8Δ60 MON1Δ1-100::natNT2-MON1pr*	This study
CUY12819	MATa *his3Δ200 leu2Δ0 met15Δ0 trp1Δ63 ura3Δ0 CCZ1::TRP1-GAL1pr CCZ1::TAP-hphNT1 mon1::kanMX GAL::pRS406-GAL1pr-MON1*	This study
CUY13278	MATa *his3Δ200 leu2Δ0 met15Δ0 trp1Δ63 ura3Δ0 CCZ1::TRP1-GAL1pr CCZ1::TAP-hphNT1 mon1::kanMX GAL::pRS406-GAL1pr-MON1 L95A L96A*	This study
CUY13882	MATa *his3Δ200 leu2Δ0 met15Δ0 trp1Δ63 ura3Δ0 CCZ1::TRP1-GAL1pr CCZ1::TAP-hphNT1 mon1::kanMX GAL::pRS406-GAL1pr-MON1 W406A*	This study
SEY6210	MATα *leu2-3,112 ura3-52 his3-Δ200 trp-Δ901 lys2-801 suc2-Δ9 GAL*	Reggiori Laboratory
CUY14281	MATα *leu2-3,112 ura3-52 his3-Δ200 trp-Δ901 lys2-801 suc2-Δ9 GAL mon1::kanMX LEU2::pRS405 MON1pr-MON1-MON1term*	This study
CUY14282	MATα *leu2-3,112 ura3-52 his3-Δ200 trp-Δ901 lys2-801 suc2-Δ9 GAL mon1::kanMX*	This study

Strains	Genotype	Reference
	LEU2::pRS405 MON1pr-MON1 W406A-Mon1term	
CUY14283	MATα *leu2-3,112 ura3-52 his3-Δ200 trp-Δ901 lys2-801 suc2-Δ9 GAL mon1::kanMX LEU2::pRS405 MON1pr-MON1 W406K-MON1term*	This study
CUY14285	MATα *leu2-3,112 ura3-52 his3-Δ200 trp-Δ901 lys2-801 suc2-Δ9 GAL mon1::kanMX LEU2::pRS405 MON1pr-MON1 L95A L96A-MON1term*	This study
CUY13605	MATα *leu2-3,112 ura3-52 his3-Δ200 trp-Δ901 lys2-801 suc2-Δ9 GAL ypt7Δ::natNT2 URA3::pRS406-YPT7pr-mNeon-(GGSG)x3-YPT7-YPT7term mon1::kanMX LEU2::pRS405 MON1pr-MON1-MON1term*	This study
CUY14287	MATα *leu2-3,112 ura3-52 his3-Δ200 trp-Δ901 lys2-801 suc2-Δ9 GAL ypt7Δ::natNT2 URA3::pRS406-YPT7pr-mNeon-(GGSG)x3-YPT7-YPT7term mon1::kanMX LEU2::pRS405 MON1pr-MON1 W406A-MON1term*	This study
CUY14288	MATα *leu2-3,112 ura3-52 his3-Δ200 trp-Δ901 lys2-801 suc2-Δ9 GAL ypt7Δ::natNT2 URA3::pRS406-YPT7pr-mNeon-(GGSG)x3-YPT7-YPT7term mon1::kanMX LEU2::pRS405 MON1pr-MON1 W406K-MON1term*	This study
CUY12706	MATα *leu2-3,112 ura3-52 his3-Δ200 trp-Δ901 lys2-801 suc2-Δ9 GAL mon1::kanMX*	This study
CUY12742	MATα *leu2-3,112 ura3-52 his3-Δ200 trp-Δ901 lys2-801 suc2-Δ9 GAL MON1pr CCZ1::mNEON-natNT2*	(2)
CUY13597	MATα *leu2-3,112 ura3-52 his3-Δ200 trp-Δ901 lys2-801 suc2-Δ9 GAL CCZ1::mNEON-natNT2 mon1::KanMX*	This study
CUY14521	MATα *leu2-3,112 ura3-52 his3-Δ200 trp-Δ901 lys2-801 suc2-Δ9 GAL MON1Δ1-100::KanMX-MON1pr CCZ1::mNEON-natNT2*	This study
CUY14522	MATalpha *leu2-3,112 ura3-52 his3-Δ200 trp-Δ901 lys2-801 suc2-Δ9 GAL mon1::kanMX LEU2::pRS405 MON1pr-MON1-MON1term CCZ1::mNEON-natNT2*	This study
CUY14523	MATα *leu2-3,112 ura3-52 his3-Δ200 trp-Δ901 lys2-801 suc2-Δ9 GAL mon1::kanMX LEU2::pRS405 MON1pr-MON1 W406A-MON1term CCZ1::mNEON-natNT2*	This study

Strains	Genotype	Reference
CUY14524	MATα *leu2-3,112 ura3-52 his3-Δ200 trp-Δ901 lys2-801 suc2-Δ9 GAL mon1::kanMX LEU2::pRS405 MON1pr-MON1 W406K-MON1term CCZ1::-mNEON-natNT2*	This study
CUY14525	MAT *leu2-3,112 ura3-52 his3-Δ200 trp-Δ901 lys2-801 suc2-Δ9 GAL mon1::kanMX LEU2::pRS405 MON1pr-MON1 L95A L96A-MON1term CCZ1::mNEON-natNT2*	This study

Table S2. Plasmids used in this study

Inserted Gene	Backbone	Reference
YPT7	pET24d-GST-TEV-	(18)
YPT10	pET24d-GST-TEV-	(18)
d.m. RAB5	pET24d-GST-TEV-	(2)
d.m. RAB7	pET24d-GST-TEV-	(2)
BET2-BET4	pCDF-DUET-1 His-TEV	(19)
MRS6	pET30	Gift from K. Alexandrov
GDI1	pGEX-6P	(19)
d.m. GDI	pET28a-His-Sumo	(2)
GST- PreSc -d.m. MON1-d.m. CCCZ1-3xFLAG-d.m.CG8270	pBig1a-	(2)
GST- PreSc -d.m. MON1 Δ1-40-*d.m.CCZ1-3xFLAG-d.m. CG8270*	pBig1a-	This study
GST- PreSc -d.m. MON1 Δ1-50-*d.m. CCZ1-3xFLAG-d.m. CG8270*	pBig1a-	This study
GST- PreSc -d.m. MON1 Δ1-100-*d.m.CCZ1-3xFLAG-d.m. CG8270*	pBig1a-	This study
GST- PreSc -d.m. MON1 I47A I48A-*d.m. CCZ1-3xFLAG- d.m. CG8270*	pBig1a-	This study
GST- PreSc -d.m. MON1 W334A-*d.m.CCZ1-3xFLAG-d.m. CG8270*	pBig1a-	This study
GST- PreSc -d.m. MON1-d.m. CCZ1-3xFLAG-d.m. CG8270-6xHIS	pBig1a-	Gift from D. Kümmel
GST- PreSc -d.m. MON1 Δ1-100-*d.m. CCZ1-3xFLAG-d.m. CG8270-6xHIS*	pBig1a-	Gift from D. Kümmel
GST- PreSc -d.m. MON1 W334A-*d.m. CCZ1-3xFLAG-d.m. CG8270-6xHIS*	pBig1a-	This study
YPT7pr-mNEON-YPT7-YPT7term	pRS406	(2)
MON1pr-MON1-MON1term	pRS405	This study
MON1pr-MON1 W406A-MON1term	pRS405	This study
MON1pr-MON1 W406K-MON1term	pRS405	This study
MON1pr-MON1 L95A L96A-MON1term	pRS405	This study
GAL1pr-MON1	pRS406	This study
GAL1pr-MON1 W406A	pRS406	This study
GAL1pr-MON1 L95A L96A	pRS406	This study

Tables S3. Kinetic constants of Rab7 GEF complexes
The following tables give an overview *of* the measured values used to calculate the fold-change in GEF-activity.

Part 1. k_{obs} values (average) for liposome GEF assays using 6.25 nM *D.m.* Mon1-Ccz1-Bulli. Related to Figure 1E and H.

Construct	k_{obs} value [s^{-1}]	STDV
Trimer wt	1,39E-03	2,94E-05
Trimer Mon1 Δ40	2,09E-03	1,16E-04
Trimer wt	1,49E-03	3,05E-04
Trimer Mon1 Δ50	3,43E-03	1,25E-03
Trimer wt	1,66E-03	5,73E-04
Trimer Mon1 Δ100	4,68E-03	1,25E-03
Trimer wt	1,87E-03	4,49E-04
Trimer Mon1 I47A I48A	2,99E-03	3,77E-04

Part 2. K_{cat}/k_m values (average) for in solution GEF assays using *D.m.* Mon1-Ccz1-Bulli. Related to Figure 1F.

Construct	k_{cat}/K_m value in solution [$M^{-1}s^{-1}$]	STDV
Trimer wt	1,49E+05	1,94E+04
Trimer Mon1 Δ100	1,58E+05	2,27E+04

Part 3. k_{obs} values (average) for liposome GEF assays using 12.5 nM *S.c.* Mon1-Ccz1. Related to Figure 2I.

Construct	k_{obs} value [s^{-1}]	STDV
wt	1,52E-03	2,55E-04
Mon1 L95A L96A	2,06E-03	1,93E-04

Part 4. K_{cat}/k_m values (average) for in solution GEF assays using *S.c.* Mon1-Ccz1. Related to Figure 2I.

Construct	k_{cat}/K_m value in solution [$M^{-1}s^{-1}$]	STDV
wt	2,45E+04	6,98E+03
Mon1 L95A L96A	2,78E+04	3,79E+03

Part 5 k_{obs} values (average) for liposome GEF assays using 25 nM *S.c.* Mon1-Ccz1. Related to Figure 3G.

Construct	k_{obs} value [s^{-1}]	STDV
wt	3,11E-03	2,11E-04
Mon1 W406A	1,80E-03	8,41E-05

Part 6 K_{cat}/k_m values (average) for in solution GEF assays using *S.c.* Mon1-Ccz1. Related to Figure 3G.

Construct	k_{cat}/K_m value in solution [$M^{-1}s^{-1}$]	STDV
wt	2,46E+04	7,11E+03
Mon1 W406A	3,03E+04	7,16E+02

Part 7 k_{obs} values (average) for liposome GEF assay using 6.25 nM *D.m.* Mon1-Ccz1-Bulli. Related to Figure 4C.

Construct	k_{obs} value [s^{-1}]	STDV
Trimer wt	2,25E-03	4,80E-04
Trimer Mon1 W334A	8,62E-04	3,28E-04

Part 8 K_{cat}/k_m values (average) for in solution GEF assay using *D.m.* Mon1-Ccz1-Bulli. Related to Figure 4C.

Construct	k_{cat}/K_m value in solution [$M^{-1}s^{-1}$]	STDV
Trimer wt	1,14E+05	3,83E+04
Trimer Mon1 W334A	1,22E+05	2,48E+04

Part 9 k_{obs} values (average) for DOGS-NTA liposome GEF assay using 25 nM *D.m.* Mon1-Ccz1-Bulli. Related to Figure S5B.

Construct	nM Rab5	k_{obs} value [s^{-1}]	STDV
Trimer wt	0	8,90E-04	1,14E-03
Trimer Mon1 Δ100	0	1,54E-03	2,21E-04
Trimer Mon1 W334A	0	6,22E-04	8,61E-04
Trimer wt	150	1,97E-03	8,58E-04
Trimer Mon1 Δ100	150	3,40E-03	1,64E-03
Trimer Mon1 W334A	150	1,65E-03	7,47E-04

Additional references for Supplemental Table S1 and S2 (19, 20)

Supplemental references

1. C. Janke, *et al.*, A versatile toolbox for PCR-based tagging of yeast genes: new fluorescent proteins, more markers and promoter substitution cassettes. *Yeast (Chichester, England)* 21, 947–962 (2004).

2. L. Langemeyer, *et al.*, A conserved and regulated mechanism drives endosomal Rab transition. *Elife* 9, e56090 (2020).

3. F. Weissmann, *et al.*, biGBac enables rapid gene assembly for the expression of large multisubunit protein complexes. *Proceedings of the National Academy of Sciences* 113, E2564–E2569 (2016).

4. M. Nordmann, *et al.*, The Mon1-Ccz1 Complex Is the GEF of the Late Endosomal Rab7 Homolog Ypt7. *Curr Biol* 20, 1654–1659 (2010).

5. L. Langemeyer, A. Perz, D. Kümmel, C. Ungermann, A guanine nucleotide exchange factor (GEF) limits Rab GTPase–driven membrane fusion. *J Biol Chem* 293, 731–739 (2018).

6. S. Kiontke, *et al.*, Architecture and mechanism of the late endosomal Rab7-like Ypt7 guanine nucleotide exchange factor complex Mon1–Ccz1. *Nat Commun* 8, 14034 (2017).

7. M. Zick, W. T. Wickner, A distinct tethering step is vital for vacuole membrane fusion. *Elife* 3, e03251 (2014).

8. R. S. Guimaraes, E. Delorme-Axford, D. J. Klionsky, F. Reggiori, Assays for the biochemical and ultrastructural measurement of selective and nonselective types of autophagy in the yeast Saccharomyces cerevisiae. *Methods* 75, 141–150 (2015).

9. J. Sellin, S. Albrecht, V. Kölsch, A. Paululat, Dynamics of heart differentiation, visualized utilizing heart enhancer elements of the Drosophila melanogaster bHLH transcription factor Hand. *Gene Expr Patterns* 6, 360–375 (2006).

10. J. Yousefian, *et al.*, Dmon1 controls recruitment of Rab7 to maturing endosomes in Drosophila. *Journal of cell science* 126, 1583–1594 (2013).

11. S. Wang, *et al.*, GBF1 (Gartenzwerg)-dependent secretion is required for Drosophila tubulogenesis. *J Cell Sci* 125, 461–472 (2012).

12. A. Paululat, J. J. Heinisch, New yeast/E. coli/Drosophila triple shuttle vectors for efficient generation of Drosophila P element transformation constructs. *Gene* 511, 300–305 (2012).

13. J. Bischof, R. K. Maeda, M. Hediger, F. Karch, K. Basler, An optimized transgenesis system for Drosophila using germ-line-specific phiC31 integrases. *P Natl Acad Sci Usa* 104, 3312–7 (2007).

14. L. Dehnen, *et al.*, A trimeric metazoan Rab7 GEF complex is crucial for endocytosis and scavenger function. *J Cell Sci* 133, jcs247080 (2020).

15. J. Schindelin, *et al.*, Fiji: an open-source platform for biological-image analysis. *Nat Methods* 9, 676–682 (2012).

16. F. Riedel, A. K. Gillingham, C. Rosa-Ferreira, A. Galindo, S. Munro, An antibody toolkit for the study of membrane traffic in Drosophila melanogaster. *Biology Open* 5, 987–992 (2016).

17. O.-E. Psathaki, L. Dehnen, P. S. Hartley, A. Paululat, Drosophila pericardial nephrocyte ultrastructure changes during ageing. *Mech Ageing Dev* 173, 9–20 (2018).

18. R. Evans, *et al.*, Protein complex prediction with AlphaFold-Multimer. *Biorxiv*, 2021.10.04.463034 (2022).

19. J. Lachmann, F. A. Barr, C. Ungermann, The Msb3/Gyp3 GAP controls the activity of the Rab GTPases Vps21 and Ypt7 at endosomes and vacuoles. *Mol Biol Cell* 23, 2516–2526 (2012).

20. L. L. Thomas, J. C. Fromme, GTPase cross talk regulates TRAPPII activation of Rab11 homologues during vesicle biogenesis. *J Cell Biol* 215, 499–513 (2016).